BMC Cancer

RESEARCH Open Access

MicroRNA-767-5p promotes metastasis but improves chemotherapeutic and radiotherapeutic sensitivity of osteosarcoma

Xuelian Luo[1,2], Xiaoyan Dai[3], Qingsong Wei[3], Xiaorong Tan[3], Shuai Wang[3], Hanxi Xiao[4], Xuan Yao[4], Youcai Deng[4*] and Zhaoyang Zhong[1*]

Abstract

The aim of this study was to explore the role of microRNA-767-5p (miR-767-5p) in regulating the osteosarcoma (OS) prognosis, metastasis and sensitivity to chemotherapeutic and radiotherapeutic sensitivity. We observed that miR-767-5p expression in the specimens of patients with metastatic OS was higher than in healthy individuals and was also negatively correlated with the overall survival of patients with OS. Functional assays (CCK-8, transwell, colony formation) and a tumor xenograft model demonstrated that miR-767-5p over-expression in both U2OS and 143B OS cell lines promoted cell invasion and migration without affecting proliferation, whereas its knockdown had opposite effects. Notably, miR-767-5p over-expression enhanced the sensitivity of both U2OS and 143B cells to chemotherapy or radiotherapy. Combing target gene prediction, RNA-sequencing and overall survival analysis, we identified aryl hydrocarbon receptor (AHR) as the potential target gene of miR-767-5p. Luciferase assay confirmed that miR-767-5p promoted the 3'-UTR activity of AHR through direct binding. Strikingly, AHR over-expression in both U2OS and 143B cells suppressed invasion, migration while reduced therapeutic sensitivity to chemotherapy and radiotherapy—thereby reversing miR-767-5p's phenotypic impact. Therefore, this study suggested that miR-767-5p promotes OS metastasis but improves its sensitivity to radiotherapy and chemotherapy.

Keywords Osteosarcoma, miR-767-5p, Aryl hydrocarbon receptor, Metastasis, Radiotherapy, Chemotherapy

*Correspondence:
Youcai Deng
youcai.deng@tmmu.edu.cn
Zhaoyang Zhong
zhongzhaoyang08@hotmail.com
[1]Department of Oncology, Hospital of Chengdu University of Traditional Chinese Medicine, Chengdu 611137, China
[2]Department of Oncology, The Third Affiliated Hospital of Chongqing Medical University (Fangda Hospital), Chongqing 401120, China
[3]Cancer Center, Daping Hospital, Army Medical University (Third Military Medical University), Chongqing 400042, China
[4]Department of Hematology, College of Pharmacy and Laboratory Medicine Science, Army Medical University (Third Military Medical University), Chongqing 400038, China

Introduction

Osteosarcoma (OS) is a rare hominin cancer, one of the most common primary malignancies of the bone, especially in children and adolescents [1]. In 1982, one randomised multi-institutional study has suggested that the 2-year actuarial progression-free survival rate is 66% among patients with OS treated with high-dose methotrexate, doxorubicin and cisplatin (MAP) after complete surgical resection [2]. Despite the emergence of multidrug chemotherapy combined with limb-sparing surgery, the survival rate of patients with OS has not significantly improved in the last three decades. Approximately 10–15% of patients newly diagnosed with OS showed metastatic diseases, especially in the lungs [1]. The 5-year survival rate is only 20% in metastasis or recurrent cases [1]. Therefore, the mechanisms of OS metastasis, recurrence and chemotherapy resistance should be explored to identify new targets for optimizing current strategies and develop new treatment methods for patients with OS.

MicroRNA (miRNA) is a subset of endogenous short non-coding RNA with a length of 20–24 nt, which forms complex networks that regulate cell differentiation, development and homeostasis [3, 4]. miRNA function dysregulation is involved in several human diseases, especially cancer [4]. Therefore, its expression could help us make earlier diagnoses and predict the prognosis, chemoresistance and radioresistance of different cancers, including OS [4, 5]. For example, several serum miRNAs have been found to act as non-invasive prognostic or diagnostic biomarkers for OS, such as miR-9, miR-21, miR-29, miR-95 and miR-194 [5, 6]. We have previously identified t miR-513a-5p and miR-765as regulators of OS chemosensitivity and radiosensitivity [7, 8]. However, the role of miRNAs in regulating OS metastasis, chemosensitivity and radiosensitivity remains largely unknown.

The aryl hydrocarbon receptor (AHR), a ligand-activated transcription factor that belongs to the periodic circadian protein (PER)–AHR nuclear translocator (AHR RNT)–single-minded protein (SIM) superfamily, integrates environmental, microbial, and metabolic signals to modulate cellular responses in cell-type-specific and context-specific manners [9]. While AHR is classically viewed as the pro-tumorigenic gene due to its mediation of pollutant-induced carcinogenesis [10, 11], its cell-type- and context-specific characteristics have led to both AHR agonists and antagonists being explored as cancer therapy [12]. AHR also modulates both innate and adaptive immune responses, suggesting a role in cancer immunology [13]. One study showed that AHR was expressed in both osteoblasts and osteoclasts, and AHR agonist 3-methylcholanthrene (3-MC) promoted oestrogen synthesis and metabolism in bone tissues [14]. The activation of AHR signalling by an agonist seemed to show agonist-type- and concentration-dependent manners in regulating OS cell proliferation and viability in vitro. For example, a 10-μM 3-MC alone did not affect the proliferation of OS cell line, i.e. MG-63 cells [14]. A 1-μM 6-Formylindolo [3,2-b] carbazole (FICZ), an AHR endogenous ligand, decreased the cell viability, whereas lower FICZ concentration improved the cell viability of MG-63 cells in vitro [15]. Exposure of MG-63 cells to AHR ligand 2,3,7,8-tetrachlorodibenzo-p-dioxin (TCDD) resulted in AHR degradation but did not affect the survival of MG-63 cells [16]. However, the cell-intrinsic role and upstream regulators of AHR in OS are still largely unknown.

Based on miRNA microarray chip analysis, a study showed that miR-767-5p is downregulated in the nasal mucosa of allergic rhinitis [17], but exhibits context-dependent roles in cancer: miR-767-5p suppresses the glioma cell growth and metastasis [18], yet promotes cell progression in multiply myeloma [19] and malignant progression in hepatocellular carcinoma [20]. A recent study evaluating the role of circular RNA has_circ_0000190 in OS found that miR-767-5p expression levels are higher in OS tumour versus normal tissues [21]. However, the direct role of miR-767-5p in regulating OS prognosis, metastasis, chemosensitivity and radiosensitivity remains largely unknown.

In this study, we demonstrate that miR-767-5p is upregulated in the OS tissues with metastasis versus non-metastasis using the clinical OS patient sample. Experimental studies reveal that miR-767-5p promotes metastasis while enhancing the sensitivity of OS cells to chemotherapy and radiotherapy both in vitro and in vivo. Mechanistically, we identify AHR as a direct miR-767-5p target and validate its dual role in OS progression and therapeutic response.

Materials and methods

Reagents and equipments

U2OS/CDDP (cisplatin resistant) were kindly provided by Professor Wei Xi, from Tianjin Cancer Hospital in 2017. Other OS cell lines used in these experiments were obtained from the Oncology Laboratory of Daping Hospital and authenticated by the Core facility of Army Medical University. All cell lines were tested to be negative for mycoplasma contamination using a Mycoplasma PCR Detection Kit (Sigma-Aldrich, Saint Louis, MO, USA) at the beginning of this project. None of the cell lines used in this study are listed in the database of commonly misidentified cell lines maintained by the International Cell Line Authentication Committee (ICLAC). Fetal bovine serum (FBS) and cell culture medium were purchased from Hyclone Laboratories (Utah, USA). Puromycin and CDDP were purchased from Sigma (St. Louis, MO, USA). PrimeScript™ RT reagent kit with gDNA eraser, TB Green® Premix Ex Taq™ II, Endonuclease NheI, and

Endonuclease SalI were purchased from Takara Bio (Dalian, China). CCK8 kits and crystal violet staining solution were purchased from Biosharp (Wuhan, China). Transwell permeable supports were obtained from BD Biosciences (Franklin Lakes, NJ, USA). A dual-Lucy assay kit was purchased from Solarbio (Beijing, China).

Tissue microarray samples

OS specimens were obtained from 86 patients with OS intra-operatively at the department of orthopaedics in Daping Hospital. This study has been carried out in accordance with the Code of Ethics of the World Medical Association (Declaration of Helsinki) for experiments involving humans and was approved by the ethics committee of Daping Hospital, Army Medical University (approval no. 2021216). All patients provided written informed consent. The clinical characteristics of patients with OS are listed in Supplementary Table 1. Kaplan–Meier analysis was used to assess the difference in the overall survival of patients with OS. A miR-767-5p expression level greater than the median value was considered high expression, while a level lower than the median value was considered low expression.

Plasmid construction and lentiviral preparation

Lentivirus overexpressing *miR-767-5p* (LV-*miR-767-5p*-OE), knockdown of *miR-767-5p* (LV-sh*miR-767-5p*), overexpressing AHR, knockdown of *AHR*and their corresponding empty vectors (LV-NC and LV-shNC) were obtained from GENECHEM (Shanghai, China). *miR-767-5p* shRNA and *AHR* shRNA sequences and the negative control are displayed in (Supplementary Table 2. PmirGLO-*AHR* 3'UTR (WT) (5'-GCAGAUAGCAAGG UUUGGUGCAA-3') and PmirGLO-*AHR* 3'UTR (Mut) (5'-GCAGAUAGCAAGGUUUCUACGTA-3') were obtained from Bioworld (Nanjing, China). The lentiviral vector pHBLV-U6-MCS-PGK-PURO (Hanbio, Shanghai, China) was used for packaging short hairpin RNA (shRNA) to knock down miR-767-5p expression [22].

Cell culture and lentivirus infection

All OS cells were cultured in RPMI 1640 medium or DMEM supplemented with 10% FBS at 37 °C in an atmosphere of 5% carbon dioxide (CO_2). OS cells were seeded in 6-well plates at a density of 2×10^5 /ml for 24 h and later infected with lentivirus expressing *miR-767-5p*, sh-*miR-767-5p*, *AHR*, sh*AHR* or their corresponding control vectors for 12 h. Subsequently, puromycin (2 μg/ml) was added to the culture medium at 37 °C with 5% CO_2 following the manufacturer's instructions to generate stable cell lines. Fluorescence microscopy, RT-qPCR and western blot assay were used to evaluate the efficiency of lentivirus transfection.

In the in vitro drug sensitivity assay, cells were cultured in CDDP-containing (2 ug/ml) medium for 24 h and then seeded into the 96-well plate at a density of 3×10^3 cells/well in culture medium, followed by the CCK-8 or colony assay at indicated time points. For in vitro radiotherapy sensitivity assays, each 6-mm cell dish was seeded with 800 cells, and 4 Gy radiotherapy was performed using a linear accelerator after cell adherence. Then, cells were placed back into the incubator to continue culturing, followed by colony formation assay at the indicated time points.

Quantitative reverse transcriptase-polymerase chain reaction (RT-qPCR) analysis

The total RNA was isolated from cells using TRIzol reagent following the manufacturer's protocol, and cDNAs were synthesised using the high-capacity cDNA reverse transcription kit (Takara Bio, Beijing, China). qPCR amplification of miR-767-5p and U6 was performed using a specific primer set. miR-767-5p expression levels were normalised to those of U6. *AHR*, *BASP1*, *FOXE1*, *AHR*, *PEG10*, *RPP25*, *ARHGEF5*, *SEMA3C* and *PLAC8* mRNA expression levels were normalised to those of GAPDH. Real-time RT-qPCR primers were designed by Pubmed Primer-BLAST and listed as in Supplementary Table 3.

Western blotting

The RIPA buffer (Solarbio, Beijing, China) containing protease inhibitors was used to extract proteins from U2OS and 143B cells. Then, a BCA kit (Solarbio, Beijing, China) was used to determine protein concentrations. Then, denatured proteins were separated by sodium dodecyl sulphate-polyacrylamide gel electrophoresis and transferred onto polyvinylidene difluoride membranes (Millipore, Billerica, USA). The membranes were blocked in Tween® 20 Detergent with 5% skim milk for 1 h and incubated with appropriate antibodies at 4 °C overnight and anti-secondary antibodies at room temperature for 1 h (all antibodies were purchased from the Cell Signalling Technology and used following the manufacturer's instructions) (Supplementary Table 4). Finally, the protein bands were detected using a Bio-Rad ChemiDoc XRS system (Bio-Rad, Hercules, CA).

CCK-8 assay

The CCK-8 assay used a CCK-8 kit (Beyotime, Shanghai, China). Cells (3×10^3 cells/well) were seeded in a 96-well plate and cultured for 18 h for adhesion. After the indicated treatment, a 10 μl of CCK8 reagent was added to each 96-well plate to detect cell proliferation ability (Beyotime, Shanghai, China) for 1 h. The absorbance was detected using a microplate reader at 450 nm.

Colony formation assay

For colony formation assay, cells in the logarithmic growth status were seeded in a 6-well plate with approximately 500 cells per well, cultured in a cell incubator at 37 °C and 5% CO_2 and saturated humidity for 2–3 weeks. Then, the medium was removed, washed with phosphate-buffered saline (PBS) three times, fixed with 4% paraformaldehyde for 15 min and stained with crystal violet solution. After rinsing, the colonies were counted under a microscope (Olympus, Japan).

Transwell assays

Approximately 2×10^4 cells in the serum-free growth medium were seeded in the upper wells of transwell chambers. The lower wells contained the same medium and were supplemented with 10% serum. After the 24-h indicated treatment, cells that migrated to the lower side of the chamber were fixed with 4% paraformaldehyde, stained with 0.1% crystal violet, dried and counted under a microscope.

RNA sequencing

The 2×10^6 LV-miR-767-5p-OE and LV-NC U2OS cells in logarithmic growth status were collected, and their total RNA was extracted using TRIzol methods and quantified using Qubit 4.0 (Invitrogen, Waltham, MA, USA). The cDNA library preparation and sequencing were performed at the Beijing Genomics Institution (Beijing, China). Concentrations and library sizes were measured using Qubit 4.0 and Agilent2100 (Agilent technologies, Santa Clara, CA, US). The cDNA library was loaded on Illumina NovaSeq 6000 (San Diego, CA, USA), and raw sequence reads in fastq format were processed and analysed, as previously described [23]. Differentially expressed genes (DEGs) were identified using Limma/voom based on raw read counts, with an adjusted *P*-value of < 0.05 and a fold change of > 2.

Prediction of the miR-767-5p target gene

Target genes of miR-767-5p were predicted through the following online websites: targetcan.org (http://www.targetscan.org), miRDB.org (http://mirdb.org/) and microRNA.org (http://www.microrna.org), and the common intersection target genes downregulated in miR-767-5p-over-expressing U2OS cells from our RNA-sequencing data were selected as the candidate target genes of miR-767-5p.

Luciferase reporter assay

Wild-type (WT) and mutated *AHR* 3'UTR were amplified and cloned into the downstream pmirGLO dual-luciferase miRNA target expression vector (Promega, Madison, Wisconsin, USA) to construct *AHR* 3′-UTR WT and Mut reporter plasmid. For dual-luciferase reporter assay, cells were cultured into 24-well plates at 4×10^3 cells per good concentration for 24 h. Then, the cells were co-transfected with *AHR* 3′-UTR WT or Mut and miR-767-5p with lipid transfection (Lipofectamine-2000 Reagent, Invitrogen). Cells were lysed after a 72-h transfection, and luciferase activity was measured by the Dual-Lucy assay kit following the manufacturer's protocol [24].

Animal experiments

Mice were obtained from Shanghai Laboratory Animal Centre. All animal experiments were performed following the National Research Council's Guide for the Care and Use of Laboratory Animals and approved by the Institutional Animal Care and Use Committee of the Army Military Medical University. Mice were subjected to dislocation under anaesthesia by 2% pentobarbital sodium before being sacrificed. To examine for metastasis, 1.0×10^6 cells from each group were suspended in 0.1 ml of PBS and injected into the lateral tail veins of 8-week-old female nude mice. At 3 and 4 weeks post-injection, living imaging of nude mice was performed using IVIS Lumina Series III (Caliper Life Sciences, Mountain View, CA, USA). Then, all mice were sacrificed, the lungs were embedded with paraffin and sliced for haematoxylin and eosin (H&E) staining and tumour foci in each section were counted. For xenograft experiments, 2×10^6 cells were subcutaneously injected into female nude mice. When tumours reached a size of approximately 100 mm^3, they were treated with CDDP or radiation. For the chemotherapy group, CDDP was injected intraperitoneally every 3 days at a concentration of 2.5 mg/g of body weight. After 25 days, the mice were sacrificed, and the tumours were excised and weighed. For the radiotherapy group, all nude mice received 4 Gy radiation each time, twice a week. Then, mice were sacrificed after four cycles of radiotherapy, and the tumours were removed and weighed.

H&E and immunohistochemistry (IHC) staining

Tumour tissues from the metastasis or xenograft model were fixed in formalin, embedded in paraffin and sectioned and followed using H&E staining. For IHC staining, sodium citrate was used for antigen retrieval, hydrogen peroxide for catalase removal and bovine serum albumin for blocking non-specific antibody binding. AHR primary antibodies were incubated overnight at 4 °C, washed three times with phosphate-buffered saline, 0.1% Tween® 20 detergent, incubated with secondary biotinylated goat anti-rabbit IgG antibody for the next 30 min and stained with diaminobenzidine (DAB), as previously described [25, 26]. Images were collected under an Olympus BX53 microscope in five random fields per sample.

Collect of public OS data and outcome analysis

The RNA-sequencing data of osteosarcoma based on TARGET (Therapeutically Applicable Research to Generate Effective Treatments) were downloaded from UCSC XENA (http://xena.ucsc.edu/). After removing patients with no information on overall survival data, a total of 85 osteosarcoma patients were selected for further analysis. Candidate miRNA-targeted genes were identified by R package survminer that using the maximally selected rank statistics to calculate the best cut-off for corresponding to the most significant relation with OS outcome. The univariate Cox regression analysis was used to further evaluate the relationship between the expression of the candidate miRNA-target genes and the OS of patients with osteosarcoma [27].

Statistical analysis

All experiments were repeated at least three times. Student's *t*-test, two-way analysis of variance (ANOVA) or one-way ANOVA was performed using GraphPad Prism 8 (GraphPad, San Diego, CA, USA), and Pearson's $\chi 2$ test was used to analyse between the miR-767-5P expression and clinical features. Data are expressed as mean ± standard deviation (S.D.). Kaplan–Meier and logrank tests were used to perform survival analysis. Univariate Cox regression analysis and likelihood ratio test were used to perform independent prognostic factors analysis. A P value < 0.05 was considered significant.

Results

miR-767-5p correlates with poor prognosis in OS patients and chemotherapeutic resistance in OS cell lines

The miR-767-5p expression levels were higher in metastatic OS samples ($n = 27$) than those without metastasis

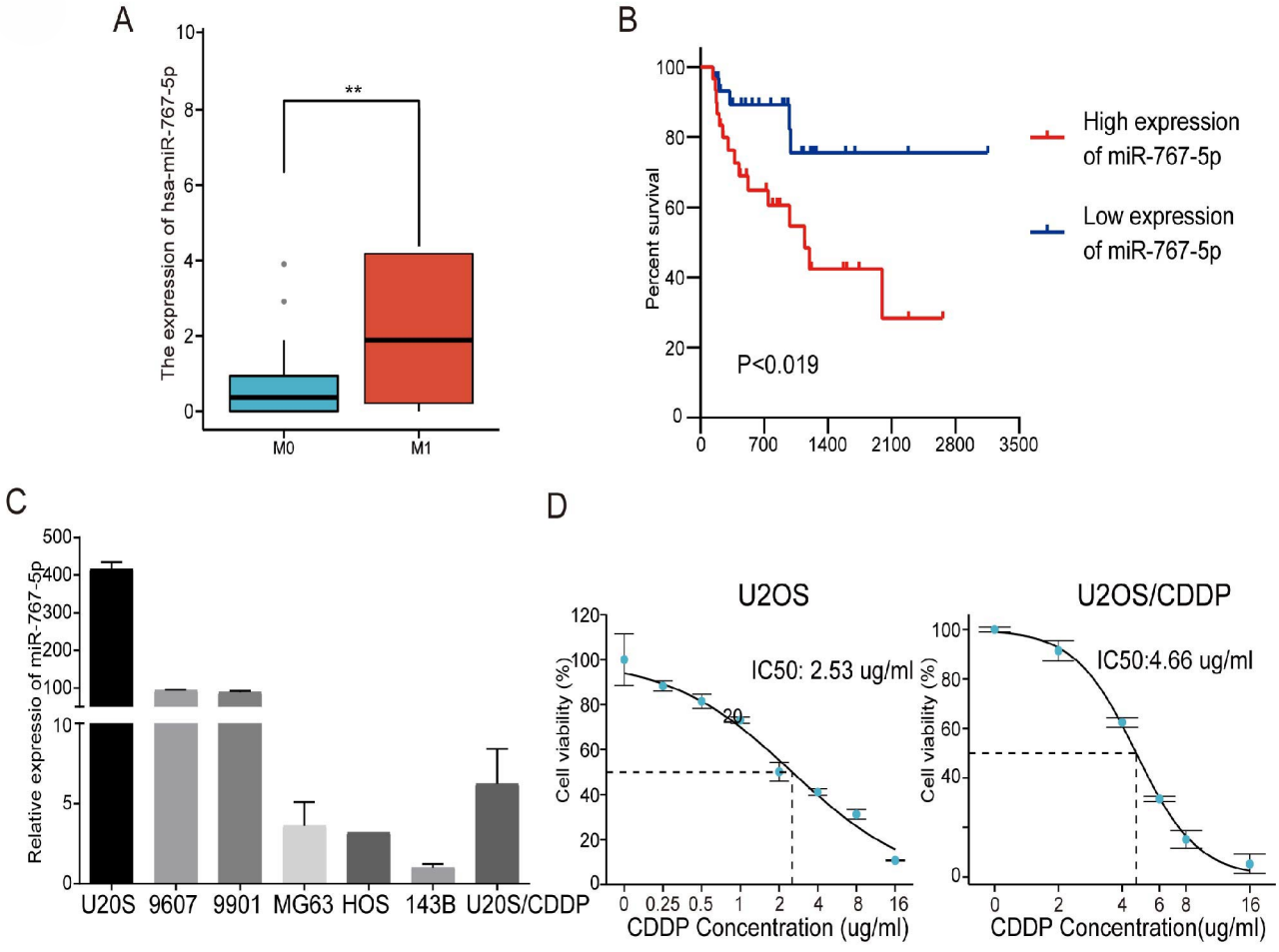

Fig. 1 miR-767-5p expression is associated with osteosarcoma metastasis and poor prognosis. **(A)** RT-qPCR analysis of miR-767-5p expression in OS patients with metastatic (M1, $n = 27$) compared to non-metastatic patients (M0, $n = 59$), $P < 0.01$ (Student's *t*-test). **(B)** Kaplan-Meier survival curves of OS patients stratified by high or low miR-767-5p expression (log-rank test). **(C)** RT-qPCR analysis of miR-767-5p levels in seven OS cell lines (U2OS, 9607, 9901, MG63, HOS, 143B, U2OS/CDDP). **(D)** IC50 of CDDP in U2OS and U2OS/CDDP cell, determined by CCK-8 assay. Data represent mean ± SD from at least three independent experiments. **, $P < 0.01$

($n = 59$) (Fig. 1A). Kaplan–Meier analysis revealed that those OS patients with relative higher miR-767-5p expression displayed worse overall survival than those OS patients with lower expression ($p < 0.05$) (Fig. 1B). The oncogenic role of miR-767-5p in the OS was further determined in various OS cell lines with different metastasis abilities, such as U2OS, U2OS/CDDP, 9607, 9901, MG63, HOS and 143B. Consistent with previous publish work [28], miR-767-5p expression was lowest in 143B cells with a significant metastatic capacity (Fig. 1C). Interestingly, we found that miR-767-5p expression in the U2OS/CDDP cells was significantly lower than that of wild-type U2OS cells (Fig. 1C). Furthermore, the CCK8 experiment was implemented to verify the effectiveness of U2OS cisplatin resistance (Fig. 1D).

All these data indicated that miR-767-5p expression was negatively correlated with the prognosis of OS patients, and positively correlated with chemotherapeutic resistance between U2OS and U2OS/CDPP cells.

miR-767-5p promotes OS cell invasion and migration but not proliferation

The RT-qPCR data confirmed that U2OS cells showed effective miR-767-5p over-expression or knockdown after infected with lentiviral vectors, whereas miR-767-5p expression levels were over-expressed by approximately 3000-fold in 143B cells, showing a relatively better capacity for in vivo tumorigenesis [28] (Fig. 2A-C). Regardless of miR-767-5p over-expression or knockdown, cell growth and proliferation were not statistically significant in both U2OS and 143B cells using CCK8 and clone formation assays for determining the cell growth and proliferation ability (Fig. 2D-I).

Furthermore, a transwell assay to assess the migration and invasion ability was conducted and found that miR-767-5p over-expression showed higher migration and invasion in both U2OS and 143B cells, whereas miR-767-5p knockdown in U2OS cells showed opposite effects (Fig. 2J-L).

All these findings supported that miR-767-5p promoted the OS cell invasion and migration, but not proliferation.

mir-767-5p enhances chemotherapeutic and radiotherapeutic sensitivities in OS cells but accelerates OS metastasis

As radiotherapy and chemotherapy are common treatments for OS, the effects of miR-767-5p on their sensitivities were further determined using CCK8 and colony assays. The CCK8 assay revealed that miR-767-5p over-expression improved cell sensitivity to CDDP treatment in both U2OS and 143B cells (Fig. 3A). To examine the miR-767-5p sensitivity to radiotherapy, colony numbers of both U2OS and 143B cells were significantly lower in miR-767-5p-over-expressed U2OS and 143B cells, as compared with their corresponding vector control cells after 4-Gy radiation (Fig. 3B). To explore the role of miR-767-5p on OS sensitivity to chemotherapy and radiotherapy in vivo, tumour xenograft was established by subcutaneously injecting miR-767-5p-over-expressed or vector control 143B cells. No significant difference was observed in the tumour volume and weight between mice injected with miR-767-5p-over-expressed and vector control 143B cells without CDDP treatment, consistent with the results that miR-767-5p did not affect the proliferation of OS in vitro. However, after the CDDP treatment for 25 days, mice injected with miR-767-5p-over-expressed 143B cells showed significantly decreased tumour size and weight than those injected with vector control 143B cells (Fig. 3C). In addition, 4-Gy radiation was performed for both mice injected with miR-767-5p-over-expressed or vector control 143B cells twice a week for 2 weeks. Data revealed that mice injected with miR-767-5p-over-expressed 143B cells had a smaller volume and lighter weight than those with vector control 143B cells (Fig. 3D). These data demonstrated that miR-767-5p is responsible for the chemotherapeutic and radiotherapeutic sensitivities in OS cells.

To further verify the role of miR-767-5p in regulating OS metastasis in vivo, miR-757-5p-over-expression or empty vector-expressed 143B cells were injected into nude mice *via* their tail veins. Our data revealed that mice injected with miR-757-5p-over-expressing 143B cells showed more metastatic nodules than the control mice in the lungs (Fig. 3E). H&E staining for lung tissues revealed that metastatic lesions in the lungs were larger in miR-767-5p-over-expressed 143B cell-injected mice than that in the control mice (Fig. 3F). Furthermore, the weight of mice injected with 143B cells over-expressing miR-767-5p was lighter than that of the control mice (Fig. 3G), which may be due to tumour metastasis aggravating the body's consumption.

Therefore, all these results demonstrate that miR-767-5p has a dichotomous role in the OS development, promoting its metastasis but improving its sensitivity to chemotherapy and radiotherapy in vivo.

AHR is a direct target gene of miR-767-5p in OS cells

Then, 3 miRNA prediction databases (targetcan, miRDB and microRNA) were used to identify the potential target genes of miR-767-5p in OS cells. Genes from the intersection of these 3 databases with DEGs between miR-767-5p-over-expression and vector control U2OS cells from our RNA sequence data were selected for further validatio, and potential 8 genes (BASP1, FOXE1, AHR, PEG10, RPP25, ARHGEF5, SEMA3C and PLAC8) were predicted from the intersection of these datasets (Fig. 4A). The mRNA expression levels of these genes

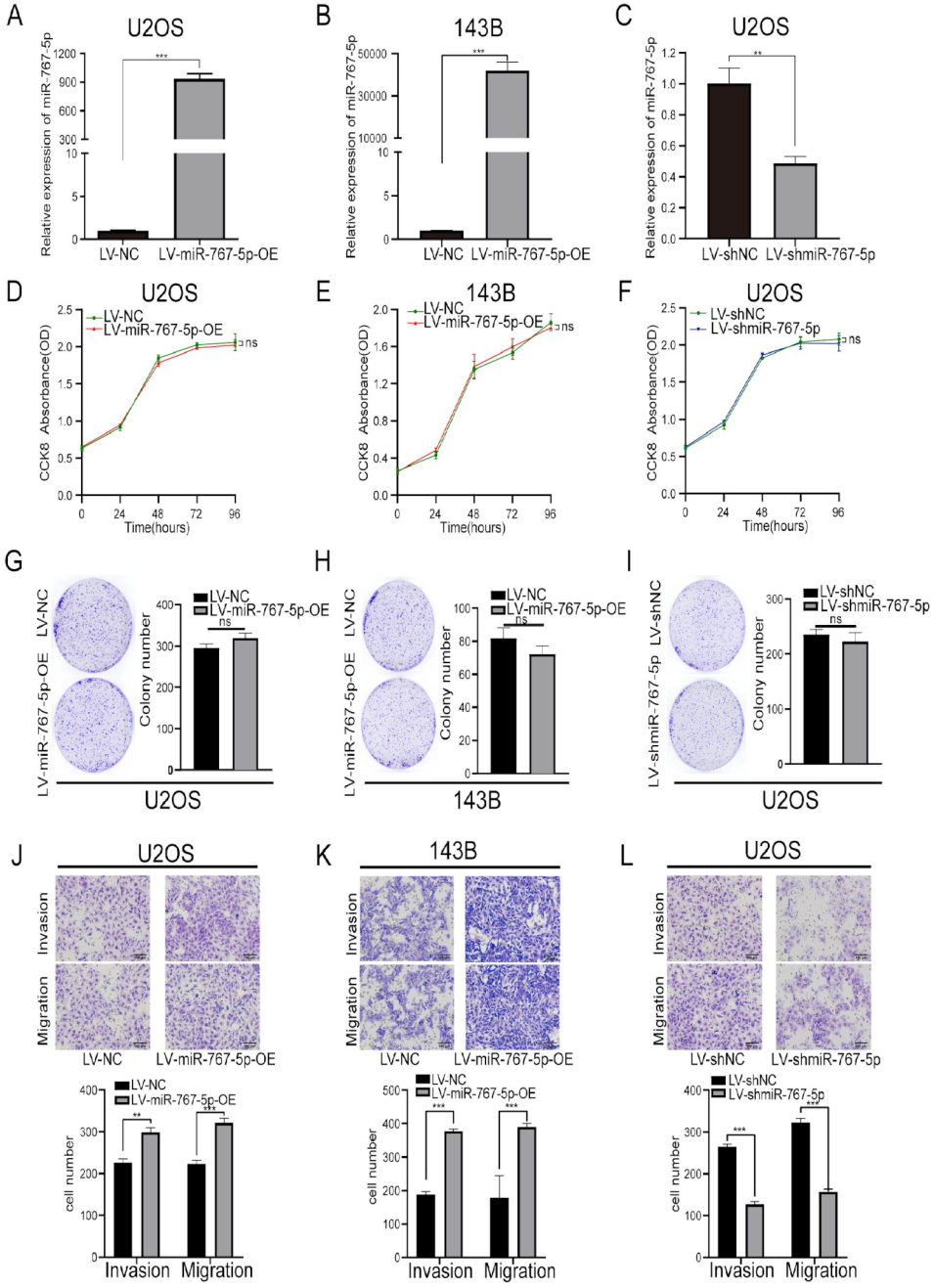

Fig. 2 miR-767-5p promotes OS cell invasion and migration but does not affect cell proliferation. **(A-C)** RT-qPCR analysis of miR-767-5p expression in U2OS **(A-B)** and 143B cells **(C)** infected with *LV-NC*, *LV-miR-767-5p-OE*, *LV-shNC* or *LV-shmiR-767-5p* (Student's *t*-test). **(D-L)** Functional assays evaluating proliferation (**D-F**, CCK8), colony formation **(G-I)** and invasion/migration (**J-L**, transwell) in U2OS and 143B cells with miR-767-5p over-expression or knock-down (Student's *t*-test). Data represent mean ± SD from at least three independent experiments. **, $P < 0.01$; ***, $P < 0.001$, ns, not significant

were further verified in both miR-767-5p-over-expressed 143B and U2OS cells using RT-qPCR. Our data showed that miR-767-5p over-expression suppressed the BASP1, FOXE1, AHR, PEG10, ARHGEF5, PLAC8 and RPP25 mRNA expressions (Fig. 4B). Similar results were found in the U2OS cells, revealing that miR-767-5p over-expression significantly inhibited the BASP1, FOXE1, AHR, PEG10, ARHGEF5, SEMA3C, PLAC8 and RPP25 mRNA expressions (Fig. 4C). We also used survival data of 85 OS patients from TARGET dataset (Therapeutically Applicable Research to Generate Effective Treatments) to explore whether the above 8 genes were involved in the prognosis of OS, such as overall survival. Kaplan–Meier and logrank tests combined with univariate Cox regression analysis revealed that only AHR could be an independent prognostic factors and lower expression AHR

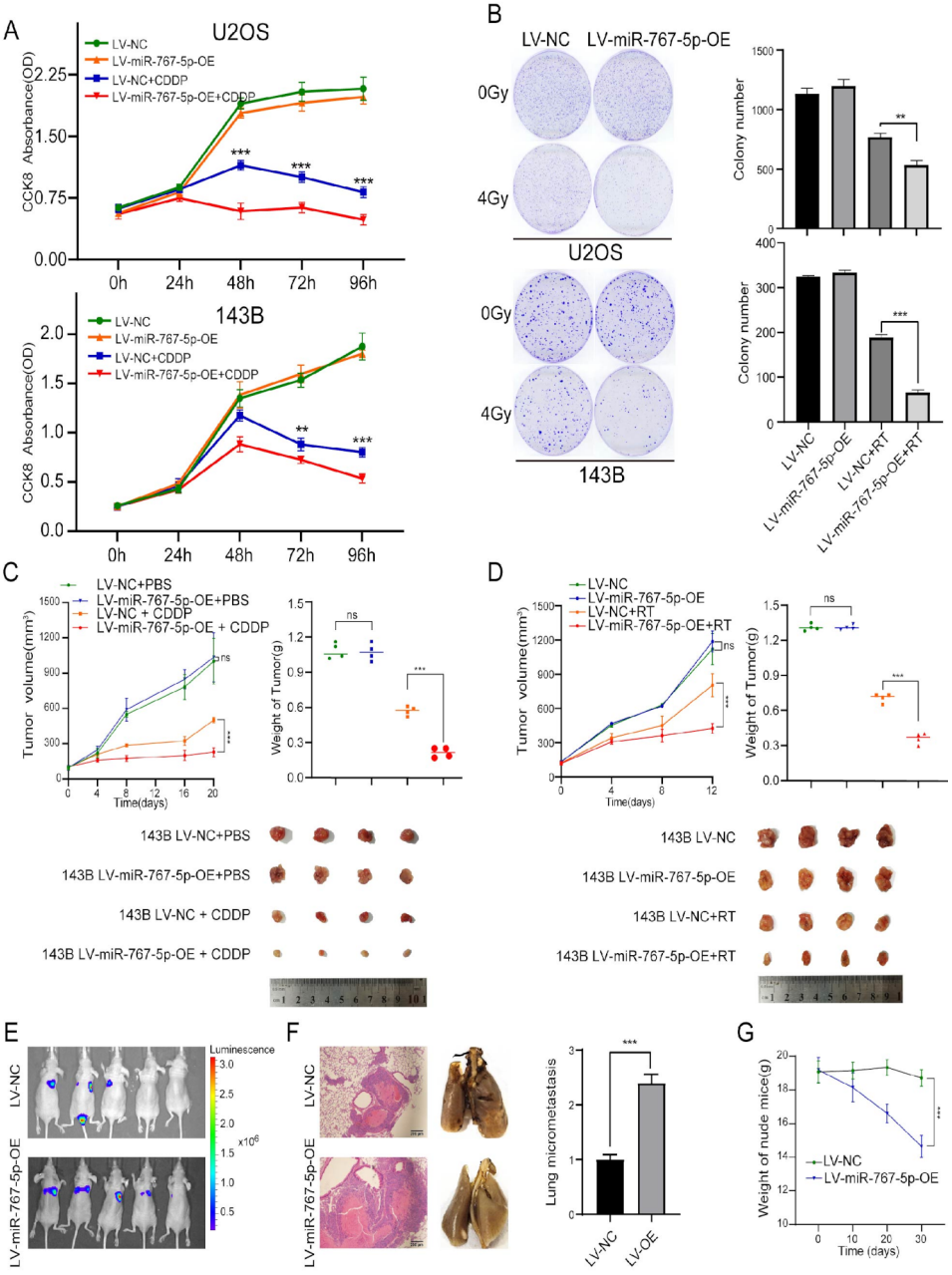

Fig. 3 MiR-767-5p increases radio- and chemotherapeutic sensitivities while promoting OS metastasis. **(A)** CCK-8 assay of proliferation in miR-767-5p-over-expressing or control U2OS (top) and 143B cells (bottom) treated with CDDP (2 μg/ml) at indicated time points (two-way ANOVA). **(B)** Colony formation assay of miR-767-5p-over-expressing or control U2OS (top) and 143B cells (bottom) after the 4-Gy radiation followed by a 2-week culture (Student's *t*-test).**(C-D)** In vivo tumor growth in nude mice subcutaneously injected with 143B cells (vector vs. miR-767-5p OE) treated with CDDP (4 mg/kg, every 3 days; **C**) or irradiation (4 Gy, twice weekly; **D**). Tumour volume (top left), tumour weight (top right) and representative images (bottom) are shown (one-way ANOVA). **(E-G)** Metastasis assay by bioluminescence imaging (E), lung H&E staining (F), and body weight monitoring (G) in nude mice injected with143B cells (vector vs. miR-767-5p OE) via tail vein. Body weights were monitored every 10 days (G) (Student's *t*-test). Data are from at least three independent experiments. ***, $P < 0.001$; ns, not significant

predicted poor prognosis of patient with OS (Fig. 4D and Supplementary Table 5).

Demonstrably, some previous studies have reported that AHR plays an important role in the migration of different tumour cells [28–30]. The potential binding site of miR-767-5p on 3'-UTR of AHR is predicted using the miRbase dataset. To provide direct experimental evidence for miR-767-5p in regulating AHR expressions, the 3'-UTR of AHR was cloned into the luciferase reporter vectors, and a parallel construct with a mutated miR-767-5p binding site was also created on AHR 3'-UTR (Fig. 4E). Data revealed that miR-767-5p restrained the

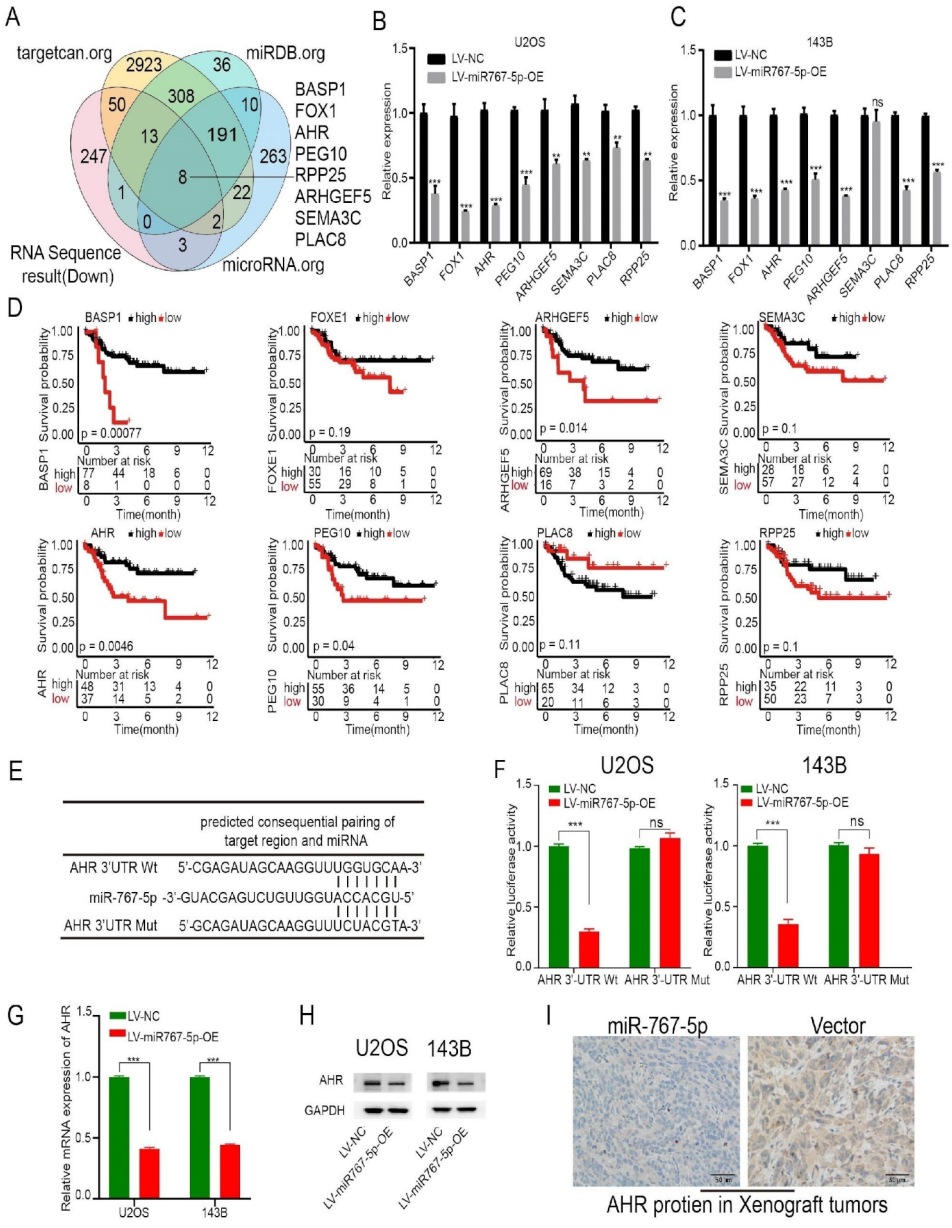

Fig. 4 Identification of AHR as a target gene of miR-767-5p in OS cells. **(A)** Venn diagram of predicted miR-767-5p targets from three miRNA databases and DEGs from RNA-seq of miR-767-5p-over-expressing U2OS cells. **(B-C)** RT-qPCR validation of eight candidate genes in miR-767-5p-over-expressing U2OS **(B)** and 143B cells **(C)** (Student's *t*-test). **(D)** Kaplan-Meier survival analysis for high/low expression of candidate genes in the TARGET dataset. **(E)** Binding site prediction of miR-767-5p on AHR 3'UTR. **(F)** Dual-luciferase assay of wild-type or mutated AHR 3'UTR activity in U2OS and 143B cells transfected with miR-767-5p or control vector (Student's *t*-test). **(G-H)** mRNA **(G)** and protein **(H)** levels of AHR in miR-767-5p-over-expressing vs. vector control U2OS or 143B cells (Student *t*-test). Western blot images were cropped from the different part of the same gel; full-length western blot images are included in the Supplementary Information. **(I)** IHC staining of AHR in xenograft tumors from143B-injected nude mice. Scale bar, 20 μm. All experiments were repeated at least three times. ***, $P < 0.001$; ns, not significant

luciferase activity of the plasmid constructed wild-type, but not mutated, AHR 3'-UTR in both 143B and U2OS cells, indicating a direct miR-767-5p binding to the 3'-UTR of AHR (Fig. 4F).

To explore whether endogenous AHR expression is affected by miR-767-5p, AHR expression, including the mRNA and protein levels, was verified in both 143B and U2OS cells that over-expressed with miR-767-5p or vector control. Both AHR mRNA and protein levels were lower in miR-767-5p over-expressing 143B and U2OS cells than those in the vector control cells (Fig. 4G-H). The AHR protein levels in the OS tissue derived from miR-767-5p-over-expressing 143B cells were significantly lower than those from vector control 143B cells (Fig. 4I).

Consequently, our study demonstrated that AHR is a direct target gene of miR-767-5p in OS cells.

AHR mediates OS progression in vitro

To explore the role of AHR in OS, AHR was further over-expressed or knocked down in both 143B and U2OS cells. RT-qPCR and western blot assay confirmed the efficiency of AHR over-expression or knockdown in AHR-over-expressed or AHR shRNA cells (Fig. 5A-B). Transwell assay revealed that AHR over-expression of AHR repressed the invasion and migration abilities of both U2OS and 143B cells (Fig. 5C and E). Conversely, AHR knockdown enhanced the invasion and migration of both U2OS and 143B cells (Fig. 5D and F).

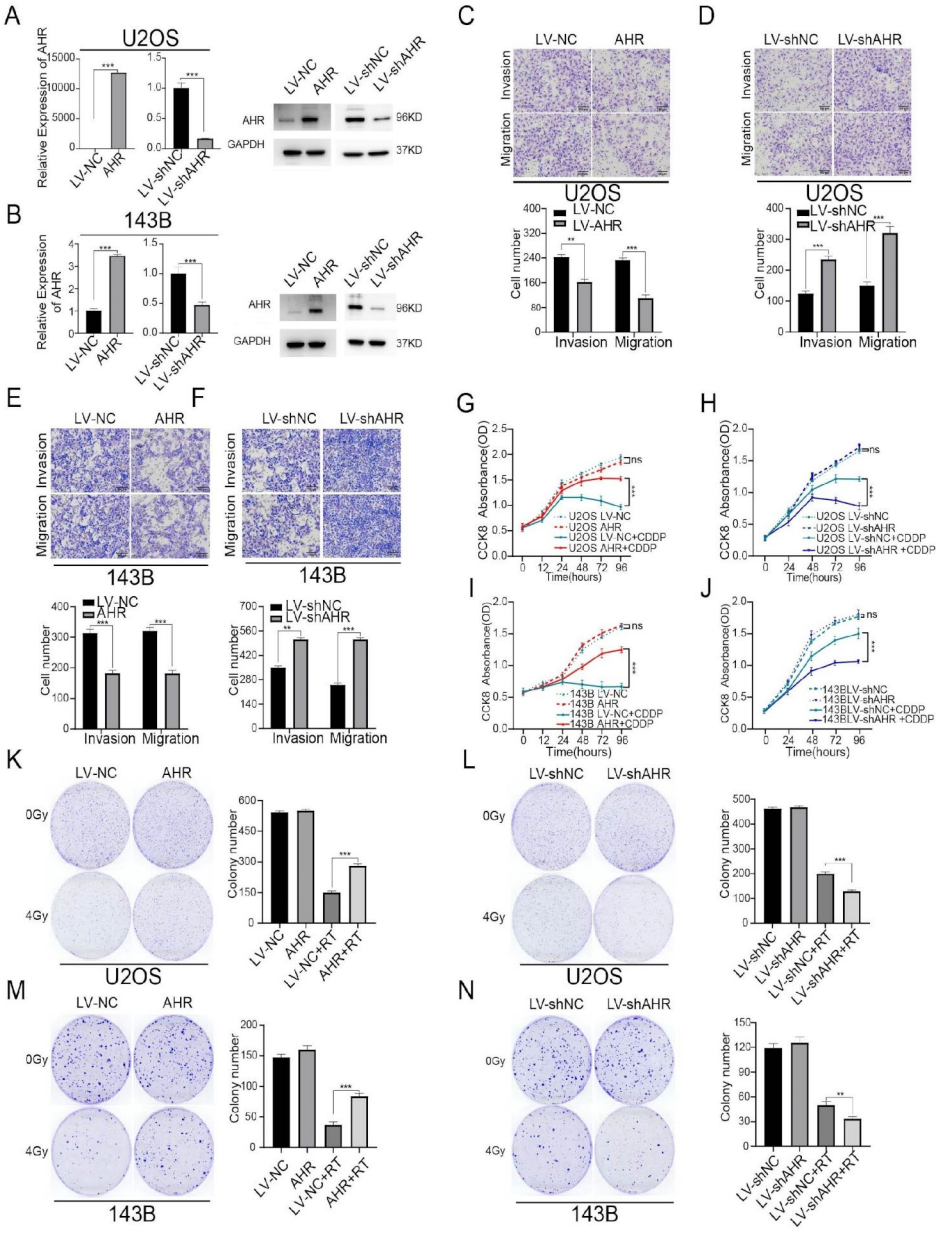

Fig. 5 AHR promotes OS invasion/migration but improves its sensitivity to chemotherapy and radiotherapy in vitro. Both U2OS and 143B cells were infected with oeAHR, shAHR and its corresponding control lentivirus. **(A-B)** The mRNA (left) and protein (right) levels of AHR in U2OS (A) and 143B **(B)** cells with oe*AHR* or sh*AHR* (vs. controls). Western blot images were cropped from the different part of the same gel; full-length western blot images are included in the Supplementary Information. **(C-F)** Colony formation assay of invasion/migration (transwell) in U2OS **(C-D)** and 143B **(E-F)** cells with oe*AHR* or sh*AHR* (vs. controls) (Student's *t*-test). **(G-J)** CCK8 assay of proliferation in U2OS **(G-H)** and 143B **(I-J)** cells with oe*AHR* or sh*AHR* (vs. controls) after CDDP (2 μg/ml) treatment at the indicated time points (two-way ANOVA). **(K-N)** Colony formation assay of invasion/migration in U2OS **(K-L)** and 143B **(M-N)** cells with oe*AHR* or sh*AHR* (vs. controls) after being exposed to 4-Gy radiation (two-way ANOVA). All experiments were repeated at least three times. Data are from at least three independent experiments. **, $P < 0.01$; ***, $P < 0.001$; ns, not significant

Furthermore, the influence of AHR on OS sensitivity to radiotherapy and chemotherapy was examined. Figure 5G-J showed that AHR over-expression or knockdown did not affect the proliferation ability of both U2OS and 143B cells. However, the cell proliferation ability was enhanced by AHR over-expression and was reduced after the AHR knockdown in both U2OS and 143B cells exposed CDDP. After exposing the mice to a dose of 4-Gy radiation, AHR over-expression increased but AHR knockdown decreased the numbers of colony formation in both U2OS and 143B cells. Interestingly, AHR over-expression or knockdown showed no effect on the numbers of colony formation at a steady state in cells without radiation (Fig. 5K-N).

Therefore, these data indicated that AHR represses OS cell invasion and migration but represses its sensitivity to radiotherapy and chemotherapy in vitro, which is highly similar to the effect of miR-767-5p in OS.

AHR over-expression reverses mir-767-5p-mediated enhanced invasion and migration but improved the OS sensitivity to chemoradiotherapy

To further explore the role of AHR in mediating the regulation of invasion, migration and sensitivity of OS to chemotherapy and radiotherapy by miR-767-5p, AHR was further over-expressed in both miR-767-5p-over-expressing 143B and U2OS cells, indicating that miR-767-5p-mediated increased invasion and migration were attenuated by AHR over-expression (Fig. 6A-B). As for the OS sensitivity to chemotherapy, our CCK-8 assay showed that AHR over-expression reversed the cell proliferation ability of miR-767-5p-over-expressed cells at post-CDDP treatment (Fig. 6C). Likewise, miR-767-5p-mediated repression of colony formation was also significantly salvaged by AHR over-expression after being exposed to 4-Gy radiation (Fig. 6D-E).

Collectively, our data demonstrated that AHR expression is independent for enhanced OS metastasis by miR-767-5p but dependent for improved sensitivity to chemoradiotherapy by miR-767-5p in OS cells.

Discussion

Different miRNAs act on diverse target genes and as tumour repressors or oncogenes. Several studies have reported the important role of various miRNAs in molecular regulation and progression of human OS [5]. Previous studies have reported different functions of miR-767-5p in tumour progression. miR-767-5p acts as oncogenes in thyroid cancer, breast cancer and hepatocellular carcinoma, but acts as a tumour repressor in glioma [18, 20, 29]. Although a previous study revealed that miR-767-5p expression was higher in OS tissues than in normal tissues and miR-767-5p directly targeted and inhibited the TET1 expression, the direct role of miR-767-5p in OS prognosis has not yet been elucidated [21]. In this study, miR-767-5p expression was found to be significantly higher in metastatic tissues than in non-metastatic tissues of OS. Although miR-767-5p did not affect the OS cell proliferation, its invasion and migration in vitro and metastasis in vivo were promoted. Interestingly, miR-767-5p improved the OS sensitivity to CDDP treatment and radiation both in vitro and in vivo, suggesting that it plays dual roles in OS, promoting metastasis but improving the therapeutic response to chemotherapy and radiotherapy.

Jia et al. have demonstrated that miR-767-5p promotes thyroid cancer cell proliferation and invasion [29]. MiR-767-5p has been reported to stimulate tumour proliferation, invasion, migration and epithelial-mesenchymal transition in breast cancer [30]. MiR-767-5p could promote proliferation, invasion and metastasis of hepatocellular carcinoma cells [20]. Conversely, the miR-767-5p expression is reduced in human glioma samples, inhibits tumour invasion and proliferation and promotes glioma cell apoptosis [18]. In our study, CCK8, clone formation and transwell experiments found that miR-767-5p promoted invasion and migration but not the proliferation of OS cells in vitro. In subcutaneous xenograft models, miR-767-5p over-expression did not affect the tumour growth, a finding consistent with the results of in vitro experiments. However, the OS metastasis model revealed that distant metastases of miR-767-5P-over-expressing OS cells were larger and higher in numbers than control OS cells. However, after radiotherapy or chemotherapy using CDDP, the tumour size of miR-767-5p-over-expressing cells was significantly reduced. All these data demonstrate that miR-767-5p promotes metastasis but strengthens the OS sensitivity to radiotherapy and chemotherapy.

Through the target gene prediction, RNA sequencing, RT-q-PCR and 767-5p binding site of 3'-UTR in AHR mutation, AHR was confirmed to be the direct target gene of miR-767-5p. Classically, AHR has been considered a pro-tumorigenic gene [13]. For instance, decreased AHR inhibits cell migration and invasion of oesophageal squamous cell carcinoma [31], glioblastoma [32] and oral squamous cell carcinoma [33]. However, AHR inhibits the migration and invasion of lung cancer cells by regulating autophagy [34]. Our data revealed that AHR over-expression in OS cells inhibited cell invasion and migration but reduced their sensitivity to radiotherapy and chemotherapy. Conversely, silencing of AHR expression in OS cells promoted cell invasion and migration and inhibited their sensitivity to radiotherapy and chemotherapy in vitro. Our study elucidates the cell-intrinsic roles of AHR in OS development and therapeutic response, repressing OS metastasis but reducing its

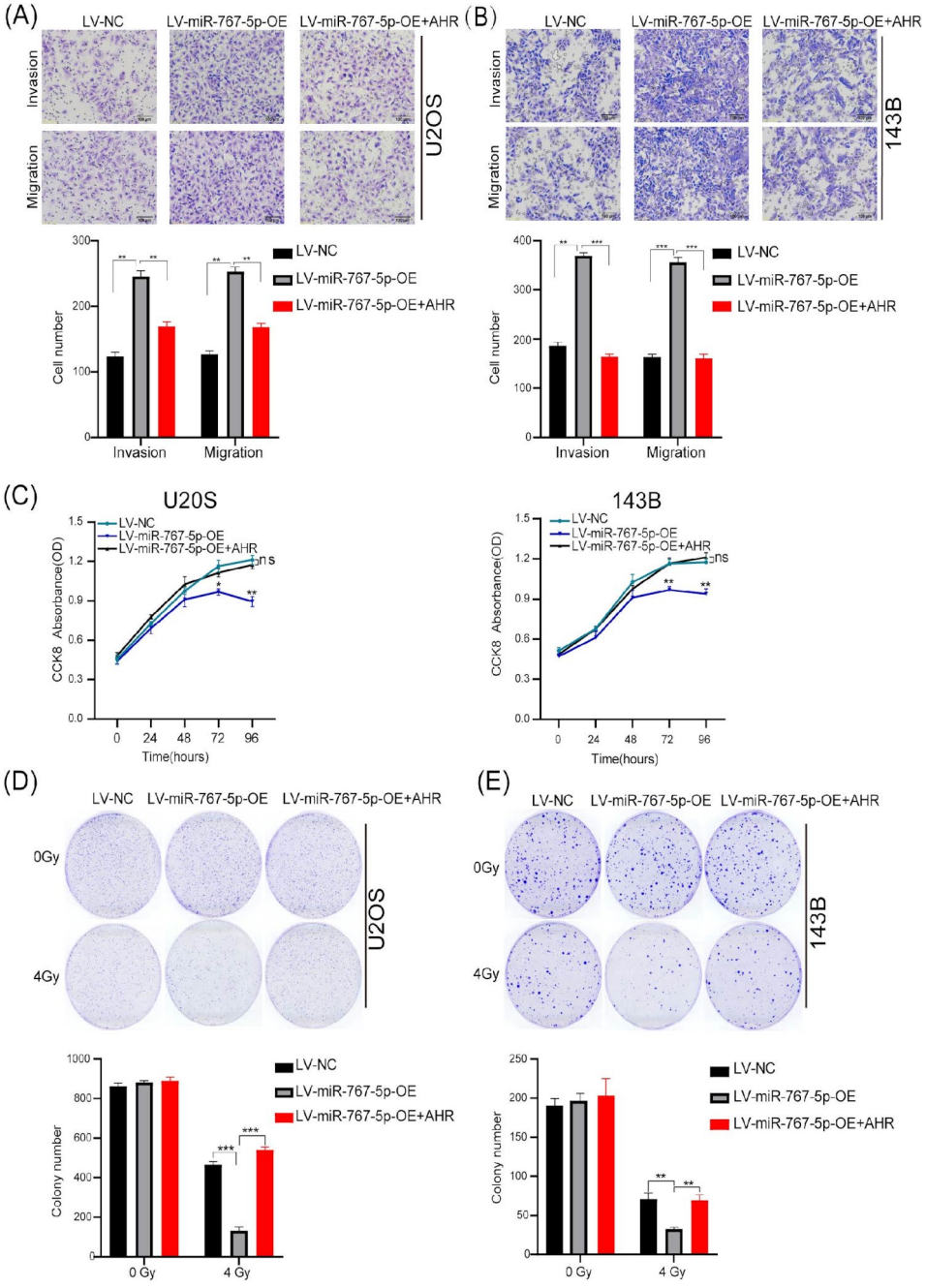

Fig. 6 AHR reverses the effects of miR-767-5p on invasion, migration and sensitivity to radiotherapy and chemotherapy in OS cells. The control vector (LV-NC), miR-767-5p-over-expressing (LV-*miR-767-5p*-OE) and miR-767-5p plus AHR co-over-expressing (LV-*miR-767-5p*OE + *AHR*) U2OS or 143B cells were established. **(A-B)** Colony assays invasion/migration in U2OS **(A)** and 143B **(B)** cells with LV-NC, LV-*miR-767-5p*-OE and LV-*miR-767-5p*-OE + AHR (one-way ANOVA). **(C)** CCK8 assays of proliferation in U2OS (left) or 143B (right) cells with LV-NC, LV-*miR-767-5p*-OE and LV-*miR-767-5p*-OE + AHR with CDDP (2 μg/ml) treatment at the indicated time points (two-way ANOVA). **(D-E)** Colony assays of invasion/migration in U2OS **(D)** and 143B **(E)** cells with LV-NC, LV-*miR-767-5p*-OE and LV-*miR-767-5p*-OE + LVAHR after being exposed to 4-Gy radiation (one-way ANOVA). All experiments were repeated at least three times. $^{**}P < 0.01$; $^{***}P < 0.001$; ns, not significant

sensitivity to radiotherapy and chemotherapy, showing an opposite effect of miR-767-5p in OS.

The mechanisms for AHR-repressing OS metastasis might be due to AHR that inhibits prostaglandin E2 (PGE2), cyclooxygenase-2 (COX2) and CXCR4 expressions. TCDD, a by-product of chlorophenols and chlorophenoxy herbicides, acts as an exogenetic ligand of AHR. A recent study revealed that TCDD could degrade the AHR protein with increased cyclooxygenase-2 (COX2), PGE2 and C-X-C motif chemokine receptor

4 (CXCR4) expressions [16]. PGE2 is a prostanoid lipid that enhanced cancer cell growth, survival, migration, invasion and immunosuppression. COX2 is the critical enzyme for PGE2 production [35]. Tumour-derived PGE2 impairs the natural killer cells stimulating the recruitment of conventional type-1 dendritic cells (cDC1) in tumour microenvironments [36]. Previous studies revealed that COX-2 or PGE2 treatment promoted U2OS cell growth, migration and invasion [37, 38]. CXCR4 is believed to promote OS progression and metastasis and is associated with poor survival of patients with OS [39, 40]. This study suggested that AHR-mediated PEG2, COX-2 or CXCR4 inhibition may play an important role in controlling OS metastasis. However, the detailed mechanisms of AHR in regulating OS cell metastasis were not investigated in this study.

Conclusions

The current study denotes that miR-767-5p is a novel biomarker that can predict the potential risk of OS metastasis and its sensitivity to radiotherapy and chemotherapy. The risk of metastasis in patients with OS with higher miR-767-5p expression was higher; however, they may have a higher sensitivity to radiotherapy and chemotherapy. The intrinsic roles and upstream regulators of AHR in OS development and therapeutic response were also elucidated for the first time, which deserves further in-depth research to discover its prognostic value and detailed mechanisms. However, this study involved with some limitations. As we did not rescue the expression of AHR in miR-767-5p knockdown OS cells, the detailed mechanism underlying AHR as a downstream target of miR-767-5p in influencing OS progression is still a little bit superficial in this work.

Abbreviations

AHR	Aryl hydrocarbon receptor
ANOVA	Analysis of variance
cDC1	Conventional type-1 dendritic cells
CDDP	Cisplatin
COX2	Cyclooxygenase-2
CXCR4	C-X-C motif chemokine receptor 4
DAB	Diaminobenzidine
FBS	Fetal bovine serum
FICZ	Formylindolo [3,2-b] carbazole
H&E	Haematoxylin and eosin
ICLAC	International cell line authentication committee
IHC	Immunohistochemistry
LV-miR-767-5p-OE	Lentivirus over-expressing miR-767-5p
LV-shmiR-767-5p	Lentivirus short hairpin microRNA-767-5p
LV-NC	Lentivirus Negative Control
LV-shNC	Lentivirus short hairpin Negative Control
MAP	Methotrexate, doxorubicin and cisplatin
miRNA	MicroRNA
OS	Osteosarcoma
PBS	Phosphate-buffered saline
PER	Periodic circadian protein
RNT	Nuclear translocator
RT-qPCR	Reverse transcriptase-polymerase chain reaction
ShRNA	Short hairpin RNA
TARGET	Therapeutically applicable research to generate effective treatments
TCDD	2,3,7,8-tetrachlorodibenzo-p-dioxin
WT	Wild-type

Supplementary Information

The online version contains supplementary material available at https://doi.org/10.1186/s12885-025-14114-y.

Supplementary Material 1

Supplementary Material 2

Acknowledgements

The author would like to thank the Core Facility of Army Medical University for living imaging.

Author contributions

This work was performed in collaboration with all authors. X.L., X.D.and Q.W. performed the experiments, analysed the data and wrote the manuscript; X.T., S.W., H.X and X.Y., collected and analysed clinical data; X.L. revised the manuscript; Y.D. designed research and wrote the manuscript; Z.Z. devised the concept, designed the research, supervised the study and wrote the manuscript.

Funding

This study was supported by grants from the Chongqing Science and Technology Commission of China (cstc2019jcyj-msxmX0502), Chongqing Municipal Education Commission Foundation (No. KJZD-M202412802 to YD), and the projects of Army Medical University (No. 2022XJS06, 2023XQN20, and 2023XQN19).

Data availability

The datasets during and/or analysed during the current study available from the corresponding author on reasonable request. All sequencing data were deposited at https://ngdc.cncb.ac.cn/gsa-human/s/d78SxHeM.

Declarations

Ethics approval and consent to participate

The study is reported in accordance with ARRIVE guidelines (https://arriveguidelines.org). The study was conducted in accordance with the Declaration of Helsinki, and approved by the Institutional Ethics Committee of Daping Hospital, Army Medical University (approval no. 2021216, Feb 16th, 2021) for studies involving humans. Informed consent was obtained from all subjects involved in the study. The animal study protocol was approved by the Institutional Ethics Committee of Daping Hospital, Army Medical University (protocol code ECAMC-2019-207, May 26th, 2019) for studies involving animals.

Consent for publication

Not applicable.

Competing interests

The authors declare no competing interests.

Received: 15 June 2023 / Accepted: 8 April 2025
Published online: 15 April 2025

References

1. Meltzer PS, Helman LJ. New horizons in the treatment of osteosarcoma. N Engl J Med. 2021;385(22):2066–76.
2. Link MP, Goorin AM, Miser AW, Green AA, Pratt CB, Belasco JB, Pritchard J, Malpas JS, Baker AR, Kirkpatrick JA, et al. The effect of adjuvant chemotherapy on relapse-free survival in patients with osteosarcoma of the extremity. N Engl J Med. 1986;314(25):1600–6.

3. Treiber T, Treiber N, Meister G. Regulation of MicroRNA biogenesis and its crosstalk with other cellular pathways. Nat Rev Mol Cell Biol. 2019;20(1):5–20.
4. Gebert LFR, MacRae IJ. Regulation of MicroRNA function in animals. Nat Rev Mol Cell Biol. 2019;20(1):21–37.
5. Llobat L, Gourbault O. Role of MicroRNAs in human osteosarcoma: future perspectives. Biomedicines. 2021;9(5).
6. Leichter AL, Sullivan MJ, Eccles MR, Chatterjee A. MicroRNA expression patterns and signalling pathways in the development and progression of childhood solid tumours. Mol Cancer. 2017;16(1):15.
7. Dai N, Qing Y, Cun Y, Zhong Z, Li C, Zhang S, Shan J, Yang X, Dai X, Cheng Y, et al. miR-513a-5p regulates radiosensitivity of osteosarcoma by targeting human apurinic/apyrimidinic endonuclease. Oncotarget. 2018;9(39):25414–26.
8. Liang W, Wei X, Li Q, Dai N, Li CY, Deng Y, Jiang X, Tan XR, Dai XY, Li MX, et al. MicroRNA-765 enhances the Anti-Angiogenic effect of CDDP via APE1 in osteosarcoma. J Cancer. 2017;8(9):1542–51.
9. Rothhammer V, Quintana FJ. The Aryl hydrocarbon receptor: an environmental sensor integrating immune responses in health and disease. Nat Rev Immunol. 2019;19(3):184–97.
10. Avilla MN, Malecki KMC, Hahn ME, Wilson RH, Bradfield CA. The ah receptor: adaptive metabolism, ligand diversity, and the xenokine model. Chem Res Toxicol. 2020;33(4):860–79.
11. Zhang W, Xie HQ, Li Y, Zhou M, Zhou Z, Wang R, Hahn ME, Zhao B. The Aryl hydrocarbon receptor: A predominant mediator for the toxicity of emerging dioxin-like compounds. J Hazard Mater. 2022;426:128084.
12. Kolluri SK, Jin UH, Safe S. Role of the Aryl hydrocarbon receptor in carcinogenesis and potential as an anti-cancer drug target. Arch Toxicol. 2017;91(7):2497–513.
13. Dean JW, Zhou L. Cell-intrinsic view of the Aryl hydrocarbon receptor in tumor immunity. Trends Immunol. 2022;43(3):245–58.
14. Miki Y, Hata S, Ono K, Suzuki T, Ito K, Kumamoto H, Sasano H. Roles of Aryl hydrocarbon receptor in Aromatase-Dependent cell proliferation in human osteoblasts. Int J Mol Sci 2017;18(10).
15. Montazeri-Najafabady N, Dabbaghmanesh MH, Chatrabnous N, Arabnezhad MR. The effects of Astaxanthin on proliferation and differentiation of MG-63 osteosarcoma cells via Aryl hydrocarbon receptor (AhR) pathway: A comparison with AhR endogenous ligand. Nutr Cancer. 2020;72(8):1400–10.
16. Yang SC, Wu CH, Tu YK, Huang SY, Chou PC. Exposure to 2,3,7,8-tetrachlorodibenzo-p-dioxin increases the activation of Aryl hydrocarbon receptor and is associated with the aggressiveness of osteosarcoma MG-63 osteoblast-like cells. Oncol Lett. 2018;16(3):3849–57.
17. Shaoqing Y, Ruxin Z, Guojun L, Zhiqiang Y, Hua H, Shudong Y, Jie Z. Microarray analysis of differentially expressed MicroRNAs in allergic rhinitis. Am J Rhinol Allergy. 2011;25(6):e242–246.
18. Zhang J, Xu S, Xu J, Li Y, Zhang J, Zhang J, Lu X. miR–767–5p inhibits glioma proliferation and metastasis by targeting SUZ12. Oncol Rep. 2019;42(1):55–66.
19. Feng Y, Zhang L, Wu J, Khadka B, Fang Z, Gu J, Tang B, Xiao R, Pan G, Liu J. CircRNA circ_0000190 inhibits the progression of multiple myeloma through modulating miR-767-5p/MAPK4 pathway. J Exp Clin Cancer Res. 2019;38(1):54.
20. Zhang L, Geng Z, Wan Y, Meng F, Meng X, Wang L. Functional analysis of miR-767-5p during the progression of hepatocellular carcinoma and the clinical relevance of its dysregulation. Histochem Cell Biol. 2020;154(2):231–43.
21. Li S, Pei Y, Wang W, Liu F, Zheng K, Zhang X. Extracellular nanovesicles-transmitted circular RNA Has_circ_0000190 suppresses osteosarcoma progression. J Cell Mol Med. 2020;24(3):2202–14.
22. Deng Y, Kerdiles Y, Chu J, Yuan S, Wang Y, Chen X, Mao H, Zhang L, Zhang J, Hughes T, et al. Transcription factor Foxo1 is a negative regulator of natural killer cell maturation and function. Immunity. 2015;42(3):457–70.
23. Yao B, Yang Q, Yang Y, Li Y, Peng H, Wu S, Wang L, Zhang S, Huang M, Wang E, et al. Screening for active compounds targeting human natural killer cell activation identifying Daphnetin as an enhancer for IFN-γ production and direct cytotoxicity. Front Immunol. 2021;12:680611.
24. Wang Y, Chu J, Yi P, Dong W, Saultz J, Wang Y, Wang H, Scoville S, Zhang J, Wu LC, et al. SMAD4 promotes TGF-β-independent NK cell homeostasis and maturation and antitumor immunity. J Clin Invest. 2018;128(11):5123–36.
25. Deng Y-F, Wu S-T, Peng H-Y, Tian L, Li Y-N, Yang Y, Meng M, Huang L-L, Xiong P-W, Li S-Y, et al. mTORC2 acts as a gatekeeper for mTORC1 deficiency-mediated impairments in ILC3 development. Acta Pharmacol Sin. 2023;44(11):2243–52.
26. Jiao J-Z, Zhang Y, Zhang W-J, He M-d, Meng M, Liu T, Ma Q-L, Xu Y, Gao P, Chen C-H, et al. Radiofrequency radiation reshapes tumor immune microenvironment into antitumor phenotype in pulmonary metastatic melanoma by inducing active transformation of tumor-infiltrating CD8 + T and NK cells. Acta Pharmacol Sin. 2024;45(7):1492–505.
27. Xiao H, Jiang N, Zhang H, Wang S, Pi Q, Chen H, He X, Luo W, Lu Y, Deng Y, et al. Inhibitors of APE1 redox and ATM synergistically sensitize osteosarcoma cells to ionizing radiation by inducing ferroptosis. Int Immunopharmacol. 2024;139:112672.
28. Mohseny AB, Machado I, Cai Y, Schaefer KL, Serra M, Hogendoorn PC, Llombart-Bosch A, Cleton-Jansen AM. Functional characterization of osteosarcoma cell lines provides representative models to study the human disease. Lab Invest. 2011;91(8):1195–205.
29. Jia M, Li Z, Pan M, Tao M, Wang J, Lu X. LINC-PINT suppresses the aggressiveness of thyroid cancer by downregulating miR-767-5p to induce TET2 expression. Mol Ther Nucleic Acids. 2020;22:319–28.
30. Wang F, Wang X, Li J, Lv P, Han M, Li L, Chen Z, Dong L, Wang N, Gu Y. Circ-NOL10 suppresses breast cancer progression by sponging miR-767-5p to regulate SOCS2/JAK/STAT signaling. J Biomed Sci. 2021;28(1):4.
31. Zhu P, Zhou K, Lu S, Bai Y, Qi R, Zhang S. Modulation of Aryl hydrocarbon receptor inhibits esophageal squamous cell carcinoma progression by repressing COX2/PGE2/STAT3 axis. J Cell Commun Signal. 2020;14(2):175–92.
32. Gramatzki D, Pantazis G, Schittenhelm J, Tabatabai G, Köhle C, Wick W, Schwarz M, Weller M, Tritschler I. Aryl hydrocarbon receptor Inhibition downregulates the TGF-beta/Smad pathway in human glioblastoma cells. Oncogene. 2009;28(28):2593–605.
33. Stanford EA, Ramirez-Cardenas A, Wang Z, Novikov O, Alamoud K, Koutrakis P, Mizgerd JP, Genco CA, Kukuruzinska M, Monti S, et al. Role for the Aryl hydrocarbon receptor and diverse ligands in oral squamous cell carcinoma migration and tumorigenesis. Mol Cancer Res. 2016;14(8):696–706.
34. Tsai CH, Li CH, Cheng YW, Lee CC, Liao PL, Lin CH, Huang SH, Kang JJ. The Inhibition of lung cancer cell migration by AhR-regulated autophagy. Sci Rep. 2017;7:41927.
35. Wang D, Dubois RN. Eicosanoids and cancer. Nat Rev Cancer. 2010;10(3):181–93.
36. Sacks D, Baxter B, Campbell BCV, Carpenter JS, Cognard C, Dippel D, Eesa M, Fischer U, Hausegger K, Hirsch JA, et al. Multisociety consensus quality improvement revised consensus statement for endovascular therapy of acute ischemic stroke. Int J Stroke. 2018;13(6):612–32.
37. Lee EJ, Choi EM, Kim SR, Park JH, Kim H, Ha KS, Kim YM, Kim SS, Choe M, Kim JI, et al. Cyclooxygenase-2 promotes cell proliferation, migration and invasion in U2OS human osteosarcoma cells. Exp Mol Med. 2007;39(4):469–76.
38. Niu JC, Ma N, Liu W, Wang PJ. EP1 receptor is involved in prostaglandin E2-induced osteosarcoma growth. Bosn J Basic Med Sci. 2019;19(3):265–73.
39. Zhu Y, Tang L, Zhao S, Sun B, Cheng L, Tang Y, Luo Z, Lin Z, Zhu J, Zhu W, et al. CXCR4-mediated osteosarcoma growth and pulmonary metastasis is suppressed by MicroRNA-613. Cancer Sci. 2018;109(8):2412–22.
40. Li YJ, Dai YL, Zhang WB, Li SJ, Tu CQ. Clinicopathological and prognostic significance of chemokine receptor CXCR4 in patients with bone and soft tissue sarcoma: a meta-analysis. Clin Exp Med. 2017;17(1):59–69.

Publisher's note